

**NASA Technical Memorandum 104212**

1N-63  
84435  
P-40

**The Double Universal Joint Wrist on a Manipulator:**

**Solution of Inverse Position Kinematics and Singularity Analysis**

(NASA-TM-104212) THE DOUBLE UNIVERSAL JOINT  
WRIST ON A MANIPULATOR: SOLUTION OF INVERSE  
POSITION KINEMATICS AND SINGULARITY ANALYSIS  
(NASA) 40 p CSCL 09B

N92-22282

Unclas  
G3/63 0084435

**Robert L. Williams II**

**March 1992**



National Aeronautics and  
Space Administration

Langley Research Center  
Hampton, VA 23665



# **THE DOUBLE UNIVERSAL JOINT WRIST ON A MANIPULATOR: SOLUTION OF INVERSE POSITION KINEMATICS AND SINGULARITY ANALYSIS**

**Dr. Robert L. Williams II  
Automation Technology Branch  
NASA Langley Research Center  
Hampton, VA 23665-5225**

## **ABSTRACT**

The double universal joint robot wrist can eliminate singularities which limit the performance of existing industrial robot wrists. Unfortunately, this singularity-free wrist has an offset which prevents decoupling of the position and orientation in the manipulator inverse kinematics problem. Closed form solutions are difficult, if not impossible, to find. This paper presents three methods to solve the inverse position kinematics position problem of the double universal joint wrist attached to a manipulator: 1) An analytical solution for two specific cases; 2) An approximate closed-form solution based on ignoring the wrist offset; and 3) An iterative method which repeats closed-form position and orientation calculations until the solution is achieved. Several manipulators are used to demonstrate the solution methods: Cartesian, cylindrical, spherical, and an anthropomorphic articulated arm, based on the the Flight Telerobotic Servicer (FTS) arm. A singularity analysis is presented for the double universal joint wrist attached to the above manipulator arms. While the double universal joint wrist standing alone is singularity-free in orientation, the singularity analysis indicates the presence of coupled position/orientation singularities of the spherical and articulated manipulators with this wrist. The Cartesian and cylindrical manipulators with the double universal joint wrist were found to be singularity free. The methods of this paper can be implemented in a real-time controller for manipulators with the double universal joint wrist. Such mechanically dextrous systems could be used in telerobotic and industrial applications, but further work is required to avoid the singularities.

## **1 INTRODUCTION**

Most existing industrial robot wrists have singularity configurations which restrict manipulator mobility. This fact adversely affects overall manipulator performance for many common industrial and telerobotic tasks. The double universal joint wrist has been proposed to eliminate wrist singularities. The kinematic diagram for this wrist is shown in Fig. 1. Singularities exist for this configuration, but mechanical limits may be designed to eliminate them and still provide a highly dextrous workspace.

Specific double universal joint wrists have been designed and built by Rosheim (1989), Milenkovic (1987), and Trevelyan, et. al. (1986). The Omni-Wrist (Rosheim, 1987) is currently used for industrial spray painting operations. The ET Wrist (Trevelyan, et. al., 1986) was designed for research in sheep shearing operations. The potential industrial and telerobotic applications for a manipulator with a double universal joint wrist are many.

Analytical solutions for the forward and inverse position and velocity kinematics of the general double universal joint wrist are presented in (Williams, 1990). This reference derives additional kinematic equations for the Omni-Wrist. The present paper studies this wrist on different manipulator arms.

The double universal joint wrist has an offset which dictates that the wrist coordinate frames cannot be located with common origins. This offset prevents decoupling of manipulator position and orientation, which complicates solution of the inverse position problem for a manipulator with this wrist. In the velocity domain, the Jacobian matrix is fully populated. Manipulators with colocated wrist frame origins have zeros in the upper right three by three portion of the Jacobian matrix.

The current paper solves the inverse position kinematics problem of the three degree of freedom double universal joint wrist on three degree of freedom Cartesian, cylindrical, spherical, and an articulated arm, based on the Flight Telerobotic Servicer (FTS) arm (see Krauze, et. al., 1990). The FTS is a seven-degree-of-freedom articulated, anthropomorphic

manipulator. In this paper, the first joint of the FTS is assumed to be locked, and the next three joints are used. The FTS wrist is replaced with the double universal joint wrist. Hereafter, the FTS is referred to as the articulated manipulator. Three inverse position solution algorithms are developed. For the Cartesian manipulator and a special case of the cylindrical manipulator, closed form solutions are found. Such analytical solutions are the exception; for most manipulators the closed form solution may not exist. The second method, the Zero Offset method, is an analytical solution. This solution results in position error because the offset is set to zero. The solution follows standard decoupling of the position and orientation. There is no orientation error. This method is good for gross motions which require little precision and/or cases where manipulator dimensions are large compared to the wrist offset. The idea for the third method, the Position/Orientation Iteration method, came from a similar method in Milenkovic(1983). A close initial guess is calculated using the Zero Offset method. The position (arm) variables and then orientation (wrist) variables are calculated, iterating until convergence to a sufficient tolerance. The methods all make use of the equations developed in (Williams, 1990).

A fourth solution method, based on iteration over forward kinematics including the Jacobian matrix (Balestrino, et. al., 1984), was considered but not pursued. The Position/Orientation Iteration method developed in the current paper is attractive for several reasons: reduced computational complexity; a good initial guess is calculated; analytical solutions are used for each position and orientation iteration; and multiple solutions are obtained.

This paper first discusses the general inverse position kinematics position problem and demonstrates why the double universal joint wrist complicates the problem. The three inverse position solution methods are then developed. The kinematic equations required for these solution methods are presented in Appendix B for the wrist and Appendix C for the Cartesian, cylindrical, spherical, and articulated arms, based on the Denavit-Hartenberg

parameters given in Appendix A. Examples are given for all of the manipulators and methods. The results section discusses an improvement on the Zero Offset method and studies the convergence of the Position/Orientation Iteration method. While the thrust of the paper is inverse position solutions, the Jacobian matrix is used for singularity study. Singularities are found to be a problem for the spherical and articulated manipulators.

## 2 SYMBOLS

<i>Arm</i>	First three joints of a 6 DOF manipulator
<i>Wrist</i>	Second three joints of a 6 DOF manipulator
$\{m\}$	Cartesian coordinate frame $m$
$\{B\}$	Manipulator base coordinate frame
$\{F\}$	Manipulator forearm coordinate frame
$\{H\}$	Manipulator hand coordinate frame
$X, Y, Z$	Cartesian arm variables
$h, \theta, r$	Cylindrical arm variables
$\theta, \phi, r$	Spherical arm variables
$\theta_1, \theta_2, \theta_3$	Articulated arm variables
$\theta_4, \theta_5, \theta_6$	Double universal joint wrist variables
${}^n_m T$	Homogeneous transformation matrix of $\{m\}$ relative to $\{n\}$
${}^B_H T$	Commanded end-effector transformation matrix
${}^B_F T$	Manipulator forearm transformation matrix
${}^F_H T$	Manipulator wrist transformation matrix
${}^n_m R$	Rotation matrix of $\{m\}$ relative to $\{n\}$
$R_{ij}$	Element (i,j) of ${}^B_H R$
$r_{ij}$	Element (i,j) of ${}^F_H R$
$\{{}^n P_m\}$	Position vector from origin of $\{n\}$ to $\{m\}$ , expressed in $\{n\}$
$(P_X, P_Y, P_Z)$	$\{{}^B P_H\}$
$\{{}^B P_H\}_E$	Approximation for $\{{}^B P_H\}$
$c_i$	$\cos \theta_i$
$s_i$	$\sin \theta_i$
$t_i$	$\tan \theta_i$
$c_{ij}$	$\cos(\theta_i + \theta_j)$
$s_{ij}$	$\sin(\theta_i + \theta_j)$
$L$	Wrist offset between the universal joints
<i>CPE</i>	Cartesian Position Error
$\epsilon$	Convergence tolerance for Position/Orientation iteration
$N$	Number of position/orientation iterations
$S$	Length of commanded position to origin
$[J]$	Six-degree-of-freedom manipulator Jacobian matrix
$[J_{AT}]$	Arm translational portion of $[J]$
$[J_{AR}]$	Arm rotational portion of $[J]$
$[J_{WT}]$	Wrist translational portion of $[J]$
$[J_{WR}]$	Wrist rotational portion of $[J]$
$\{\dot{\theta}\}$	Vector of six joint rates
$\{\dot{X}\}$	Cartesian translational and rotational velocities
$\{\dot{X}_1\}$	Arm contribution to Cartesian velocities
$\{\dot{X}_2\}$	Wrist contribution to Cartesian velocities

### **3 THE INVERSE POSITION KINEMATICS PROBLEM**

The forward kinematics problem is a mapping,  $f$ , from joint space,  $\theta$  to Cartesian space,  $y$ . For serial manipulators, the forward kinematics problem is straightforward.

$$y = f(\theta) \quad (1)$$

The inverse position kinematics problem inverts Eq. 1, mapping the Cartesian space to joint space. Equation 2 is generally difficult to solve because the system is coupled, transcendental, and multiple solutions generally exist.

$$\theta = f^{-1}(y) \quad (2)$$

This section discusses the general inverse position kinematics problem for a manipulator arm and wrist combination. Two cases are considered: For wrists with three co-located coordinate frames the position and orientation may be decoupled. For double universal joint wrists and other wrists without co-located coordinate frames this decoupling is not available, which reduces the possibility of a closed-form solution.

The forward kinematics solution may be expressed as a concatenation of homogeneous transformation matrices, partitioned in the following at the forearm frame.

$$[{}^B_H T] = [{}^B_F T(\theta_1, \theta_2, \theta_3)] [{}^F_H T(\theta_5, \theta_6, \theta_6)] \quad (3)$$

The inverse position kinematics problem uses the same equation, but  $[{}^B_H T]$  is specified and the joint angles are unknown.

$$[{}^B_H T] = \begin{bmatrix} R_{11} & R_{12} & R_{13} & P_X \\ R_{21} & R_{22} & R_{23} & P_Y \\ R_{31} & R_{32} & R_{33} & P_Z \\ 0 & 0 & 0 & 1 \end{bmatrix} \quad (4)$$

#### **3.1 Manipulator Wrists with Co-located Frames**

Most common industrial wrists are designed to be purely rotational, with three co-incident frames. The vector from the forearm frame to the hand frame is zero in this



case. Pieper (1968) proved that if a manipulator has any three consecutive frames with coincident origins, a closed-form solution exists. This solution is found for many common manipulators by decoupling the Cartesian position and orientation. The forearm frame origin is always co-located with the hand frame origin, and so the Cartesian position is only a function of  $(\theta_1, \theta_2, \theta_3)$ . This is seen by applying Eq. 3, with  $\{^F P_H\} = 0$ .

$$[{}^B_H T] = \left[ \begin{array}{c|c} [{}^B_F R] & \{^B P_F\} \\ \hline 0 & 1 \end{array} \right] \left[ \begin{array}{c|c} [{}^F_H R] & \{0\} \\ \hline 0 & 1 \end{array} \right] = \left[ \begin{array}{c|c} [{}^B_H R] & \{^B P_F\} \\ \hline 0 & 1 \end{array} \right] \quad (5)$$

$$\begin{Bmatrix} P_X \\ P_Y \\ P_Z \end{Bmatrix} = \{^B P_F(\theta_1, \theta_2, \theta_3)\} \quad (6)$$

After solving  $(\theta_1, \theta_2, \theta_3)$ ,  $[{}^B_F R]$  is known, from which  $[{}^F_H R]$  is formed.

$$[{}^F_H R] = [{}^B_F R]^{-1} [{}^B_H R] \quad (7)$$

With  $[{}^F_H R]$  known, the wrist angles  $(\theta_4, \theta_5, \theta_6)$  are found by inverting the appropriate Euler angle set.

### 3.2 Double Universal Joint Wrist

For the double universal joint wrist and other wrists which do not have co-located frames, the position and orientation problem is coupled. This is because  $\{^F P_H\}$  is non-zero;  $\{^F P_H\}$  is the fourth column of  $[{}^F_H T]$  (see Eq. B.1). When the method above is applied for such wrists, Eq. 6 has the following form.

$$\begin{Bmatrix} P_X \\ P_Y \\ P_Z \end{Bmatrix} = \{^B P_H(\theta_1, \theta_2, \theta_3, \theta_4, \theta_5, \theta_6)\} \quad (8)$$

Three more equations are required (from the orientation); the resulting six equations are transcendental and fully coupled in the six unknowns. A closed-form solution for this case is generally elusive.

The following equation is an attempt to obtain an equation in the form of Eq. 6.

$$\{^B P_F\} = \{^B P_H\} - [{}^B_F R] \{^F P_H\} \quad (9)$$

This attempt fails because  $\{^F P_H\}$  depends on unknowns  $(\theta_4, \theta_5, \theta_6)$ .

The inverse position solution is not necessarily the best algorithm for a manipulator with the double universal joint wrist. The resolved motion rate solution (Whitney (Brady, et. al., 1982)) is an attractive alternative. The resolved motion rate kinematics solution for control of instantaneous end-effector velocity is advantageous for many reasons. Two main reasons are: 1) the solution is linear and unique, assuming the Jacobian matrix has full rank. 2) inputs from position, vision, force, hand controller, and other control elements may be summed linearly (weighted) to obtain simultaneous mixed-mode control. However, this paper concentrates on the inverse position problem.

## 4 INVERSE POSITION KINEMATICS SOLUTION METHODS

Three methods were used to solve the inverse position kinematics of the manipulators in Figs. 2a - 2d with the double universal joint wrist. Closed-form solutions were found for two manipulators. No analytic solutions were found for the remaining manipulators. The Zero Offset and Position/Orientation Iteration methods were applied to manipulators with no analytical solution.

Figures 2a through 2d show the four arms with three freedoms each. Each arm has a base frame  $\{B\}$  and a forearm frame  $\{F\}$  where the double universal joint wrist of Fig.1 is mounted. The end-effector frame is  $\{H\}$  in Fig. 1. The kinematic terms used in the inverse position solution methods are given in Appendices. Appendix A gives Denavit-Hartenberg parameters (Denavit and Hartenberg, 1955) for the Cartesian, cylindrical, spherical, and articulated arms, and the double universal joint wrist. A summary of the double universal joint wrist forward and inverse position kinematics solutions, plus the Jacobian matrix, are presented in Appendix B, derived from Williams (1990). Appendix C gives the forward and inverse kinematics solutions for the Cartesian, cylindrical, spherical, and articulated arms, each having three-degrees-of-freedom.

### 4.1 Closed-Form Solutions

An analytical solution was developed for the Cartesian manipulator. The basis for this solution is that  ${}^B_F R = [I]$  for all  $(X, Y, Z)$ . With this information, Eq. 7 yields:

$${}^F_H R = {}^B_H R \quad (10)$$

With  ${}^F_H R$  known, the wrist angles are calculated with Eqs. B.2a through B.2c, given in Appendix B. Once the wrist angles are known the wrist offset may be accounted for by using Eq. 9 to calculate the Cartesian joint values  $(X, Y, Z)$ .

$$\begin{aligned} \{{}^B P_F\} &= \{{}^B P_H\} - \{{}^F P_H\} \\ \begin{Bmatrix} X \\ Y \\ Z \end{Bmatrix} &= \begin{Bmatrix} P_X \\ P_Y \\ P_Z \end{Bmatrix} - \begin{Bmatrix} LK_1 \\ LK_2 \\ Lc_5c_6 \end{Bmatrix} \end{aligned} \quad (11)$$

Where  $K_1$  and  $K_2$  are defined in Eq. B.1.

A closed-form solution for the cylindrical I manipulator of Fig. 2b was attempted. Though this attempt failed, an analytical solution was found for the cylindrical II manipulator. The difference between the cylindrical I and II manipulators is the mounting orientation of the double universal joint wrist, as seen in Fig. 2b. For either cylindrical manipulator,  ${}^B_F R$  is a function of the unknown  $\theta_2$ . Therefore, Eq. 7 may not be applied to solve  $(\theta_4, \theta_5, \theta_6)$  first, as in the Cartesian case. Rather, the kinematics equations, Eq. 3, are used to solve for  $(h, \theta, r)$  first. The key to the solution is the following combination of the wrist unknowns  $(\theta_5, \theta_6)$ , where  $R_{32}$  is given.

$$c_5 c_6 = \sqrt{\frac{r_{32} + 1}{2}} \quad (12)$$

Using Eq. 12, the position and orientation is decoupled. The solution is:

$$h = P_Z - L c_5 c_6 \quad (13a)$$

$$\theta = \tan^{-1} \left( \frac{B}{A} \right) \quad (13b)$$

$$r = \sqrt{A^2 + B^2} \quad (13c)$$

where:

$$A = P_X - \frac{L r_{12}}{2 c_5 c_6}$$

$$B = P_Y - \frac{L r_{22}}{2 c_5 c_6}$$

There is a unique solution, assuming  $R > 0$  and using a quadrant-specific inverse tangent function.

Following the position solution above, Eq. 7 is used to find  ${}^B_H R$  with which Eqs. B.2a through B.2c yield  $(\theta_4, \theta_5, \theta_6)$ .

## 4.2 Zero Offset Method

The closed-form solutions presented in the previous section are for special cases. For general manipulators with the double universal joint wrist, the offset  $L$  prevents decoupling

of the position unknowns and the orientation unknowns  $\theta_4, \theta_5, \theta_6$ . The Zero Offset method solves the inverse position kinematics problem by assuming  $L = 0$ . Closed-form solutions result, but there is positioning error. The assumption for this method is that  $L$  is small relative to the other manipulator dimensions.

Figure 3 shows the flow chart for the Zero Offset method, encased in dotted lines. The assumption  $L = 0$  forces all wrist frame origins to be co-located with the  $\{F\}$  origin and the following is true:

$$\{{}^B P_F\} = \{{}^B P_H\} \quad (14)$$

With this condition, the solution method follows Eqs. 5, 6, and 7. The solutions for the first three joints given  $(P_X, P_Y, P_Z)$  are given in the Appendix C for the cylindrical, spherical, and articulated arms. After solving the first three joint values, the wrist angles are solved from Eqs. B.2a through B.2c, given  ${}^E_H R$  from Eq. 7.

A benefit of this method is that the orientation error is zero. The  $(\theta_4, \theta_5, \theta_6)$  values are not the exact solution. However, they produce the exact commanded orientation because they are based on  ${}^B_F R$  (calculated from the first three joints which are in error due to  $L = 0$ ) and the original  ${}^B_H R$ .

The position vector error resulting from the Zero Offset method is expressed by the scalar Cartesian position error (CPE). The commanded position vector is  $\{{}^B P_H\}$ ; the actual position vector is  $\{{}^B P_H\}_E$ , calculated by forward kinematics with the first three joint values from the Zero Offset method. The Euclidean norm is used in Eq. 15.

$$CPE = \|\{{}^B P_H\} - \{{}^B P_H\}_E\| \quad (15)$$

### 4.3 Position/Orientation Iteration Method

The Position/Orientation Iteration method for solving the inverse position kinematics of a manipulator with non-co-located wrist axes is an extension of the Zero Offset method. The flow chart for the Position/Orientation Iteration algorithm is shown in Fig. 3.

To start the process, the offset  $L$  is assumed to be zero, which leads to Eq. 14. Given this  $\{{}^B P_F\}$ , the position unknowns are found and then the orientation unknowns  $(\theta_4, \theta_5, \theta_6)$  are solved in the same manner as the Zero Offset method.

Equation 9 is used to obtain a better value for  $\{{}^B P_F\}$  than the zero-offset assumption yields. This equation may be applied because approximate values for the joints have been calculated. The updated  $\{{}^B P_F\}$  is used to repeat the calculations, solving the position and then wrist unknowns. By using Eq. 9, the zero-offset assumption is no longer required, and  $\{{}^B P_H\}_E$  rapidly converges to  $\{{}^B P_H\}$ . The algorithm terminates when CPE is below a specified tolerance  $\epsilon$ .

The Position/Orientation Iteration method has several strong points. The convergence is rapid and assured when  $L$  is small relative to other manipulator dimensions. No initial guess is required; the starting point is calculated by assuming zero offset. While the overall scheme is numerical, the position and orientation solutions are analytical. Due to this fact, all possible solutions are given, where most numerical techniques track only one solution.

## 5 EXAMPLES

This section gives inverse position kinematics examples for the methods and equations presented in Section 4. Closed-form solutions are available for the Cartesian and cylindrical II manipulators. For the cylindrical I, spherical, and articulated manipulators, examples are given for the Zero Offset and Position/Orientation Iteration methods.

Units for the examples are meters for length and degrees for angles. The position error (CPE) is given in millimeters. The articulated manipulator dimensions are  $L_1 = 0.230$ ,  $L_2 = 0.560$ , and  $L_3 = 0.555$ . The prismatic joints for the Cartesian, cylindrical, and spherical manipulators are allowed enough range to reach the articulated manipulator workspace. Angular limits are not considered. All manipulators have the double universal joint wrist with  $L = 41 \text{ mm}$  which is taken from the commercial wrist in (Rosheim, 1987). For the Position/Orientation Iteration method,  $\epsilon = 1 \text{ mm}$ ;  $N$  is the number of iterations for convergence. As derived in Appendix C, the spherical arm has two and the articulated arm four inverse position solutions.

For all examples, the input command is:

$${}^B_H T = \begin{bmatrix} -0.211 & -0.480 & -0.852 & 0.600 \\ 0.857 & 0.328 & -0.397 & 0.300 \\ 0.470 & -0.814 & 0.342 & 0.600 \\ 0 & 0 & 0 & 1 \end{bmatrix} \quad (16)$$

### 5.1 Closed-Form Solutions

#### Cartesian Manipulator

X	Y	Z	$\theta_4$	$\theta_5$	$\theta_6$	CPE
0.632	0.278	0.587	-88.5	68.4	-34.0	0

#### Cylindrical II Manipulator

h	$\theta$	r	$\theta_4$	$\theta_5$	$\theta_6$	CPE
0.587	23.7	0.691	-112.2	68.4	-34.0	0

## 5.2 Zero Offset Method

### Cylindrical I Manipulator

h	$\theta$	r	$\theta_4$	$\theta_5$	$\theta_6$	CPE
0.600	26.6	0.671	-46.3	15.2	51.6	41

### Spherical Manipulator

$\theta$	$\phi$	r	$\theta_4$	$\theta_5$	$\theta_6$	CPE
26.6	41.8	0.900	4.7	61.7	42.2	41
206.6	138.2	0.900	184.7	61.7	42.2	41

### Articulated Manipulator

$\theta_1$	$\theta_2$	$\theta_3$	$\theta_4$	$\theta_5$	$\theta_6$	CPE
26.6	102.0	255.6	132.1	13.2	51.0	41
26.6	5.4	-271.0	-13.8	65.2	-39.4	41
206.6	161.2	-37.5	41.5	71.5	24.2	41
206.6	131.4	22.1	-20.7	44.9	51.7	41

## 5.3 Position/Orientation Iteration Method

### Cylindrical I Manipulator

h	$\theta$	r	$\theta_4$	$\theta_5$	$\theta_6$	CPE	N
0.628	25.0	0.646	-48.1	13.7	52.4	0.84	2

### Spherical Manipulator

$\theta$	$\phi$	r	$\theta_4$	$\theta_5$	$\theta_6$	CPE	N
23.9	43.4	0.886	6.5	63.2	42.6	0.89	2
203.9	136.6	0.886	186.5	63.2	42.6	0.89	2



### Articulated Manipulator

$\theta_1$	$\theta_2$	$\theta_3$	$\theta_4$	$\theta_5$	$\theta_6$	CPE	N
25.1	104.2	-103.2	132.8	14.7	52.6	0.02	3
23.8	3.7	88.5	-16.5	66.8	-36.8	0.19	3
203.3	163.8	-43.2	52.5	73.5	20.2	0.36	3
204.6	127.3	27.1	-23.8	43.0	53.6	0.09	3

For the Closed-Form solutions CPE is zero, assuming ideal kinematics. The Zero Offset method always has  $CPE = L$ , which is 41 *mm* in this example. The final CPE for the Position/Orientation Iteration examples is smaller than  $\epsilon = 1$  *mm*; many cases are significantly smaller. Convergence was obtained in two or three iterations for all manipulators.

## 6 INVERSE POSITION KINEMATICS RESULTS

In this section, an improvement on the Zero Offset method and its effect on the articulated manipulator is studied. Also, the Position/Orientation Iteration method convergence is presented for a specific command to the cylindrical I, spherical, and articulated manipulators.

As demonstrated in the examples, the solution for any manipulator using the Zero Offset method always yields  $CPE = L$ , the double universal joint wrist offset. A simple modification of the method is attempted to reduce this error without additional calculation or using Position/Orientation Iteration. The offset is still set to zero, so that  $\{H\}$  is collocated with  $\{F\}$ . However, three values for  $L_3$  are considered: 1)  $L_3 = L_0$ , the original case; 2)  $L_3 = L_0 + \frac{L}{2}$ ; and 3)  $L_3 = L_0 + L$ ;

This modification may be applied to all of the manipulators in this paper. Results are reported in Fig. 4 for the articulated manipulator. The input command is:

$${}^B_H T = \begin{bmatrix} -0.211 & -0.480 & -0.852 & 0.667S \\ 0.857 & 0.328 & -0.397 & 0.333S \\ 0.470 & -0.814 & 0.342 & 0.667S \\ 0 & 0 & 0 & 1 \end{bmatrix} \quad (17)$$

The orientation is fixed; CPE is studied for commanded reaches of 0.30, 0.60, 0.90, and 1.20 m ( $S = 0.30, 0.60, 0.90, 1.20$  m in Eq. 17) from the origin, along the unit vector direction  $\{0.667, 0.333, 0.667\}^T$ . The average CPE from multiple solutions is reported.

The horizontal line on Fig. 4 represents the Zero Offset method results, with a constant  $CPE = 41$  mm. The other two lines ( $\{F\}$  origin shifts of  $\frac{L}{2}$  and  $L$ ) show that significant error reduction is achieved by the modified Zero Offset method for shorter reaches. However, the modified method can yield errors greater than the wrist offset for longer reaches. In conclusion, the modified Zero Offset method can give better results for the same computational effort, but regions exist where the results may be worse.

Figure 5 shows the convergence of the Position/Orientation Iteration method for the cylindrical, spherical, and articulated manipulators. The input command is Eq. 16. For

each iteration, CPE decreases approximately by an order of magnitude. The first iteration is the same as the Zero Offset method; hence,  $CPE = 41 \text{ mm}$  for all manipulators. After the second iteration, all errors are about  $1 \text{ mm}$ , and after three iterations all errors are significantly less than  $0.1 \text{ mm}$ . Therefore, for telerobotic and industrial tasks, two or three iterations are sufficient for these manipulators. The calculations required at each iteration are relatively few due to the use of analytical solutions given in Appendices B and C. The methods of this paper should be implementable in a real-time controller for manipulators.

## 7 MANIPULATOR SINGULARITY ANALYSIS

Manipulator singularities may be found mathematically via the determinant of the manipulator Jacobian matrix. This paper has presented position methods thus far; the Jacobian matrix is in the velocity domain. All joint angle sets which result in zero or near zero determinant are at or near singular configurations. Singularities arise from workspace boundaries and other workspace conditions which instantaneously cause the loss of a degree of freedom, such as two or more manipulator joint axes aligning. In the neighborhood of singularities, a finite Cartesian velocity command requires joint velocities approaching infinity. The result is that the commanded Cartesian velocity cannot be achieved when the manipulator configuration is near a singularity.

For manipulators with a spherical wrist mechanism, singularities may be classified as arm singularities and wrist singularities. Under such cases, the Jacobian matrix is of the following form. The position and orientation components are decoupled, as discussed in Section 3.1. In Eq. 18, the subscripts  $A, W, T, R$  stand for Arm, Wrist, Translational, and Rotational, respectively. Each sub-matrix of Eq. 18 has order three by three.

$${}^0[J] = \left[ \begin{array}{c|c} [J_{AT}] & [0] \\ \hline [J_{AR}] & [J_{WR}] \end{array} \right] \quad (18)$$

The arm singularities are found from  $|J_{AT}| = 0$  and wrist singularities from  $|J_{WR}| = 0$ .

For a manipulator with a non-spherical wrist mechanism, such as the double universal joint wrist, the Jacobian matrix is fully populated. That is,  $[J_{WT}]$ , the upper right quadrant of Eq. 18, is not equal to the zero matrix. The double universal joint wrist alone is singularity-free (Rosheim, 1987, and Williams, 1990). Any singularities existing for the first three joints also exist for the overall manipulator. The following question arises: Are there any singularities due to the coupling of position and orientation? In other words, are there any wrist joint sets which cause singularities for the overall manipulator? This

question is answered by analyzing the determinant of the complete Jacobian matrices for each manipulator that includes the double universal joint wrist mechanism. The full six by six determinant is studied because of the position and orientation coupling.

## 7.1 Manipulator Jacobian Matrices

The Jacobian matrix is a linear operator which maps joint space velocities to Cartesian velocities. In Eq. 19,  $m$  is the coordinate frame that the Cartesian velocities and Jacobian matrix are expressed in.

$$m\{\dot{X}\} = m[J]\{\dot{\theta}\} \quad (19)$$

For six axis manipulators operating in a six dimensional task space (three translations and three rotations),  $m[J]$  is a square matrix of order six. A method is presented in this section to determine this overall manipulator Jacobian matrix by combining the arm wrist Jacobian matrices.

The arm joint Jacobian matrix represents the translational and rotational Cartesian velocity components due to the arm joints. The vector  $\{\dot{X}_1\}$  contains the linear and angular velocities of  $\{F\}$  with respect to  $\{B\}$ , expressed in any coordinate frame (assume  $\{B\}$  for this section). The symbolic terms for the various arm joint Jacobian matrices are not presented. They are readily obtained using the Denavit-Hartenberg parameters of Appendix A and any Jacobian matrix derivation method (for example, see Whitney (Brady, et. al., 1982), Paul (1982), or Craig (1986)). The Denavit-Hartenberg parameters in Appendix A are based on Craig's notation (1986).

$$\{\dot{X}_1\} = \begin{bmatrix} {}^B[J_{AT}] \\ - - - \\ {}^B[J_{AR}] \end{bmatrix} \begin{Bmatrix} \dot{\theta}_1 \\ \dot{\theta}_2 \\ \dot{\theta}_3 \end{Bmatrix} \quad (20)$$

The Cartesian velocity vector  $\{\dot{X}_2\}$  contains the linear and angular velocities of  $\{H\}$  with respect to  $\{F\}$ , expressed in  $\{H\}$  in this paper. This accounts for the translational

and rotational Cartesian velocity components due to the wrist joints.

$$\{\dot{X}_2\} = \begin{bmatrix} {}^H[J_{WT}] \\ - - - \\ {}^H[J_{WR}] \end{bmatrix} \begin{Bmatrix} \dot{\theta}_4 \\ \dot{\theta}_5 \\ \dot{\theta}_6 \end{Bmatrix} \quad (21)$$

The matrices  ${}^H[J_{WT}]$  and  ${}^H[J_{WR}]$  are given in Eqs. B.3a and B.3b of Appendix B.

The overall manipulator Jacobian matrix  $[J]$  is found with the relative velocity equation, Eq. 22; both velocity vectors must be expressed in the same frame. The Jacobian matrix is assumed to be expressed in  $\{B\}$ ; therefore, the wrist Jacobian matrices are transformed as shown.

$$\dot{x} = \{\dot{X}_1\} + \{\dot{X}_2\} \quad (22)$$

$$[J] = \begin{bmatrix} {}^B[J_{AT}] & | & [{}^B_R]{}^H[J_{WT}] \\ - - - & | & - - - \\ {}^B[J_{AR}] & | & [{}^B_R]{}^H[J_{WR}] \end{bmatrix} \quad (23)$$

## 7.2 Manipulator Singularity Conditions

Singularity conditions are reported below for the manipulators studied in this paper. The symbolic overall Jacobian matrix determinants are presented for the Cartesian, cylindrical I, cylindrical II, and spherical manipulators with the double universal joint wrist. The articulated manipulator determinant was derived symbolically but is not given because of its complexity. Equating the determinant of  $[J]$  to zero yields the singularity conditions.

The Jacobian matrix determinant for the Cartesian manipulator with the wrist is Eq. 24.

$$|J| = 4c_5c_6^2 = 0 \quad (24)$$

Due to the simple structure of the Cartesian manipulator, Eq. 24 is identical to the rotational Jacobian matrix (Eq. B.3b) determinant of the wrist standing alone (Williams, 1990). The singularity conditions are solved by inspection,  $\theta_5 = \pm 90^\circ$  or  $\theta_6 = \pm 90^\circ$ . If the wrist is designed such that these angles are out of the mechanical wrist workspace, the Cartesian manipulator with the wrist is singularity free. The commercial wrist in Rosheim

(1987) has limits  $-45^\circ < \theta_5, \theta_6 < 45^\circ$ , and still achieves a large nominally hemispherical workspace.

As the manipulator complexity increases, the symbolic form of the Jacobian matrix determinant grows, and less is evident from the determinant structure. The remaining manipulator with wrist singularity conditions are derived via an exhaustive multi-dimensional numerical search for small determinant. Partial analytical results are given for the cylindrical I, cylindrical II, and spherical manipulators. These determinants each have a factored multiple of  $c_6$  (Eqs. 25, 26, and 27). Thus,  $\theta_6 = \pm 90^\circ$  is a singularity condition for these three manipulators with the wrist.

For the cylindrical I and cylindrical II manipulators, respectively, the determinants are given below.

$$|J| = 2rc_6^2[-s\theta s_5 s_6 - 2c_5 + c\theta c_6] = 0 \quad (25)$$

$$|J| = 2rc_6^2[s\theta s_5 s_6 - 2c_5] = 0 \quad (26)$$

Both cylindrical manipulators with the wrist are singularity-free. The angle  $\theta$  was varied over a revolution, while  $\theta_5, \theta_6$  were varied over  $\pm 50^\circ$ , all with one degree steps. No determinant was less than 0.2 for either case. The cylindrical manipulators both have singularities for  $r = 0$ , but this is assumed to be out of the workspace. Several coupled singularities were found at general wrist angle values, but all were out of the commercial wrist workspace mentioned above.

The Jacobian matrix determinant for the spherical manipulator is Eq. 27.

$$|J| = c_6[4r^2 c\phi c_5 c_6^2 + 2rs\phi(1 - s_5^2 c_6^2) + c\phi c_5 s_6 c_6 + s\phi s_6] = 0 \quad (27)$$

The determinant above is zero for  $r = 0$  and  $\phi = 0$  or  $\theta_6 = 0$ , but  $r = 0$  is assumed to be out of the workspace. The spherical manipulator yields many coupled singularities throughout the workspace of the manipulator and wrist. The singular conditions occur at general angular values, and are non-intuitive.

The articulated manipulator Jacobian matrix determinant is not given due to the complexity. The behavior of the articulated manipulator with wrist is similar to that of the Spherical manipulator. There are many coupled position/orientation singularities existing at various locations within the workspace. Locations for these singularities are difficult, if not impossible to predict analytically.

### **7.3 Manipulator Singularity Summary**

For simple manipulator structures such as the Cartesian manipulator and both cylindrical manipulators, the double universal joint wrist does not cause coupled singularities. Therefore, these overall manipulators are singularity-free, preserving a benefit of the wrist (ignoring workspace limit singularities). As the manipulator structure becomes more complex, coupled position/orientation singularities arise, at locations difficult to predict off-line.

A possible singularity remedy is to calculate the overall manipulator Jacobian matrix determinant for each time step. If the determinant is zero or small, the Moore-Penrose pseudoinverse (Noble, 1966) may be used instead of standard numeric or symbolic matrix inversion. The resulting motion will not track the command exactly near a singularity, but will enable smooth motion out of the singular region.



## **8 CONCLUSION**

This paper presents methods to solve the inverse position kinematics problem, plus a singularity analysis of the double universal joint wrist on a manipulator. The offset of this singularity-free wrist prevents decoupling of the position and orientation. The theory is applied to Cartesian, cylindrical, spherical, and articulated manipulators.

Closed form solutions are found for the Cartesian and cylindrical II manipulators. The Zero Offset method is a closed form solution, but has an associated positioning error. The orientation error is zero, assuming ideal kinematics. This method may be used for gross motions, assuming that the wrist offset is small relative to the other manipulator dimensions. The modified Zero Offset method presented in the Section 6 can reduce this error significantly; however, longer manipulator reaches can increase the error.

The Position/Orientation Iteration method is iterative, but each step uses analytical solutions. It was found that two iterations are sufficient for most industrial and telerobotic requirements, using the manipulators in this paper. Three iterations allows high precision; the resulting error is smaller than the physical system uncertainties and backlash. No initial guess is required, multiple solutions are found, and the method is efficient.

A manipulator singularity analysis was performed using the Jacobian matrices of the Cartesian, cylindrical I and II, spherical, and articulated arms with the double universal joint wrist. It was found that the Cartesian and cylindrical manipulators are singularity free when using the wrist. Singularities were found at many non-intuitive locations for the spherical and articulated manipulators. This is a potentially serious limitation of the wrist, used on common manipulator structures.

## **9 REFERENCES**

Balestrino, A., De Maria, G., and Sciavicco, L., "Robust Control of Robotic Manipulators", *Proceedings of the 9th IFAC World Congress*, Budapest, Hungary, July, 1984.

Craig, J.J., **Introduction to Robotics: Mechanics and Control**, Addison Wesley Publishing Co., Reading, MA, 1988.

Denavit, J., and Hartenberg, R.S., "A Kinematic Notation for Lower Pair Mechanisms Based on Matrices", *Journal of Applied Mechanics, Trans. ASME*, Vol. 77, June 1955, pp. 215-221.

Krauze, L.D., Schlagel, J.H., and Henry, P.L., "Space Station Telerobotic Servicer (FTS) Phase C/D DTF-1 Manipulator/End Effector Kinematic Analysis", Final Report, Contract NAS5-30689, Martin Marietta Astronautics Group, August, 1990.

Milenkovic, V., "New Nonsingular Robot Wrist Design", *Robots 11 Conference Proceedings RI/SME*, Chicago, IL, April 1987, pp. 13.29-13.42.

Milenkovic, V., and Huang, B., "Kinematics of Major Robot Linkage", *Robots 7 Conference Proceedings RI/SME*, Chicago, IL, April 1983, pp. 16.31 - 16.42.

Noble, B., Daniel, J.W., **Applied Linear Algebra**, Prentice-Hall, Inc., Englewood Cliffs, NJ, 1966, pp. 338-339.

Paul, R.P., **Robot Manipulators: Mathematics, Planning, and Control**, The MIT Press, Cambridge, MA, 1982.

Pieper, D., "The Kinematics of Manipulators Under Computer Control", Ph.D. Thesis, Stanford University, 1968.

Rosheim, M.E., **Robot Wrist Actuators**, John Wiley & Sons, New York, 1989.

Rosheim, M.E., "Singularity-Free Hollow Spray Painting Wrists", *Robots 11 Conference Proceedings RI/SME*, Chicago, IL, April 1987, pp. 13.7-13.28.

Trevelyan, J.P., et. al., "ET: A Wrist Mechanism Without Singular Positions", *The International Journal of Robotics Research*, Winter, 1986, pp. 71-85.

Whitney, D.E., "The Mathematics of Coordinated Control of Prosthetic Arms and Manipulators", **Robot Motion: Planning and Control**, Brady, M., Hollerbach, J.M., Johnson, T., Lozano-Perez, T., and Mason, M., editors, The MIT Press, Cambridge, MA, 1982, pp. 287-304.

Williams, R. L., "Forward and Inverse Kinematics of Double Universal Joint Robot Wrists", *Proceedings of the 1990 Space Operations, Applications, and Research (SOAR) Symposium*, June 26-28, 1990, Albuquerque, NM.

## **APPENDIX A: DENAVIT-HARTENBERG PARAMETERS**

This appendix presents the Denavit-Hartenberg parameters (Denavit and Hartenberg, 1955) for the three-axis Cartesian, cylindrical I and II, spherical, and articulated arms of Figs. 2a - 2d. The parameters describe manipulator links and joints in a standard manner, based on the notation of Craig (1986). The Denavit-Hartenberg parameters are also given for the double universal joint wrist from Williams (1990). The wrist parameter table, Table A.5, has five lines of parameters. However, there are only three degrees-of-freedom due to the coupling of wrist joint angles.

To obtain the overall manipulator parameters, parameters  $i = 4$  through  $H$  are appended to the parameters of the selected three degree-of-freedom arm. The wrist base frame in Williams (1990) is  $\{F\}$  in this paper. For the articulated arm parameters,  $\{F\}$  is defined as shown in order to make use of the wrist frames in Williams (1990). No variable exists on line  $F$  in Table A.4. The remaining manipulators mount the wrist so  $\{F\}$  is the same as the third coordinate frame. For the examples in Section 5 and the kinematic equations in Appendix C,  $L_4 = 0$  in Table A.4.

**Table A.1: Cartesian Arm Parameters**

$i$	$\alpha_{i-1}$	$a_{i-1}$	$d_i$	$\theta_i$
1	0	X	0	$90^\circ$
2	0	Y	0	$-90^\circ$
3	0	0	Z	0

**Table A.2a: Cylindrical I Arm Parameters**

$i$	$\alpha_{i-1}$	$a_{i-1}$	$d_i$	$\theta_i$
1	0	0	h	0
2	0	0	0	$\theta + 90^\circ$
3	$90^\circ$	0	r	0

**Table A.2b: Cylindrical II Arm Parameters**

i	$\alpha_{i-1}$	$a_{i-1}$	$d_i$	$\theta_i$
1	0	0	h	0
2	0	0	0	$\theta$
3	0	r	0	0

**Table A.3: Spherical Arm Parameters**

i	$\alpha_{i-1}$	$a_{i-1}$	$d_i$	$\theta_i$
1	0	0	0	$\theta$
2	$90^\circ$	0	0	$\phi + 90^\circ$
3	$90^\circ$	0	r	0

**Table A.4: Articulated Arm Parameters**

i	$\alpha_{i-1}$	$a_{i-1}$	$d_i$	$\theta_i$
1	0	0	0	$\theta_1$
2	$90^\circ$	$L_1$	0	$\theta_2$
3	0	$L_2$	0	$\theta_3 + 90^\circ$
F	$90^\circ$	$L_4$	$L_3$	$90^\circ$

**Table A.5: Double Universal Joint Wrist Parameters**

i	$\alpha_{i-1}$	$a_{i-1}$	$d_i$	$\theta_i$
4	0	0	0	$\theta_4 + 90^\circ$
5	$90^\circ$	0	0	$\theta_5 + 90^\circ$
6	$90^\circ$	0	0	$\theta_6$
7	0	L	0	$\theta_6$
H	$-90^\circ$	0	0	$\theta_5 - 90^\circ$

## APPENDIX B: DOUBLE UNIVERSAL JOINT WRIST KINEMATICS

A kinematic diagram of the general double universal joint wrist is shown in Fig. 1. Williams (1990) presents forward and inverse position and velocity kinematics both for the general wrist and a commercially-available wrist of this kinematic structure. This reference gives equations for the wrist standing alone, i.e. relating  $\{H\}$  to  $\{F\}$ . The forward and inverse position solutions are summarized below for use in the larger inverse position kinematics solution for a double universal joint wrist mounted on a three degree of freedom manipulator arm. The wrist Jacobian matrix is also given, for use in singularity analysis, Section 7.

The forward position solution forms  ${}^F_H T$  given  $(\theta_4, \theta_5, \theta_6)$ .

$${}^F_H T = \begin{bmatrix} 2s_5c_6K_1 - s_4 & 2c_5c_6K_1 & -2s_6K_1 + c_4 & L(K_1) \\ 2s_5c_6K_2 + c_4 & 2c_5c_6K_2 & -2s_6K_2 + s_4 & L(K_2) \\ 2s_5c_5c_6^2 & 2c_5^2c_6^2 - 1 & -2c_5s_6c_6 & Lc_5c_6 \\ 0 & 0 & 0 & 1 \end{bmatrix} \quad (B.1)$$

$$K_1 = c_4s_6 + s_4s_5c_6$$

$$K_2 = s_4s_6 - c_4s_5c_6$$

Due to the offset  $L$  between the two universal joints,  $\{F P_H\}$  is non-zero.

The inverse position kinematics solution finds  $(\theta_4, \theta_5, \theta_6)$  given  ${}^F_H R$ . The full  ${}^F_H T$  cannot be specified because it has six freedoms.

$$\theta_4 = 2\tan^{-1} \left[ \frac{-F}{G-E} \right] \quad (B.2a)$$

$$\theta_5 = \tan^{-1} \left[ \frac{r_{13}s_4 - r_{23}c_4}{r_{33}} \right] \quad (B.2b)$$

$$\theta_6 = \frac{1}{2}\tan^{-1} \left[ \frac{(r_{23}c_4 - r_{13}s_4)s_5 - r_{33}c_5}{r_{13}c_4 + r_{23}s_4} \right] \quad (B.2c)$$

where:

$$E = -(r_{13} + r_{21})$$

$$F = r_{11} - r_{23}$$

$$G = r_{32} + 1$$

Due to symmetry, there are four solutions, summarized in Table B.1.

**Table B.1: Wrist Inverse Position Solutions**

Solution	$\theta_4$	$\theta_5$	$\theta_6$
1	$\theta_4$	$\theta_5$	$\theta_6$
2	$\theta_4$	$\theta_5$	$\theta_6 + \pi$
3	$\theta_4$	$\theta_5 + \pi$	$-\theta_6$
4	$\theta_4$	$\theta_5 + \pi$	$-\theta_6 + \pi$

The commercial wrist detailed in (Rosheim, 1987) has angular limits  $-45^\circ < \theta_5, \theta_6 < 45^\circ$ .

Therefore, only the first line of Table I is a viable solution.

For the double universal joint wrist standing alone, the Jacobian matrix order is six by three. Three joint rates are mapped to six Cartesian velocity terms, three translational and three rotational. The Jacobian matrix for the wrist is reported below, with respect to  $\{H\}$  coordinates, where  ${}^H[J_{WT}]$  is the translational part and  ${}^H[J_{WR}]$  the rotational part.

$${}^H[J_{WT}] = L \begin{bmatrix} s_6 & -c_5 c_6 & s_5 s_6 \\ 0 & s_5 c_6 & c_5 s_6 \\ s_5 c_6 & 0 & c_6 \end{bmatrix} \quad (B.3a)$$

$${}^H[J_{WR}] = \begin{bmatrix} s_2 \theta_5 c_6^2 & s_5 s_2 \theta_6 & 2c_5 \\ 2c_5^2 c_6^2 - 1 & c_5 s_2 \theta_6 & -2s_5 \\ -c_5 s_2 \theta_6 & 2c_6^2 & 0 \end{bmatrix} \quad (B.3b)$$

For spherical wrists,  $[J_{WR}] = [0]$ . The matrix  ${}^H[J_{WR}]$  above demonstrates the coupling between position and orientation.

## APPENDIX C: MANIPULATOR POSITION KINEMATICS

This appendix presents position kinematics for the first three joints of the cylindrical I, spherical, and articulated manipulators, pictured in Figs. 2b - 2d. For each manipulator, the forward kinematics solution  ${}^B_F T$  is given. Also, the inverse position kinematics problem is solved: given  ${}^B P_F$ , calculate values for the first three joints. These solutions are used along with the wrist solutions (Eqs. B.2a through B.2c) in the Zero Offset and Position/Orientation Iteration methods described in Sections 4.2 and 4.3, respectively. The inverse position solution for the three-axis Cartesian manipulator is presented in Section 4.1.

### C.1 Cylindrical I Manipulator

$${}^B_F T = \begin{bmatrix} -s\theta & 0 & c\theta & rc\theta \\ c\theta & 0 & s\theta & rs\theta \\ 0 & 1 & 0 & h \\ 0 & 0 & 0 & 1 \end{bmatrix} \quad (C.1)$$

$$h = P_Z \quad (C.2a)$$

$$\theta = \tan^{-1} \left( \frac{P_Y}{P_X} \right) \quad (C.2b)$$

$$r = \sqrt{P_X^2 + P_Y^2} \quad (C.2c)$$

There is one solution, assuming positive  $r$ .

### C.2 Spherical Manipulator

$${}^B_F T = \begin{bmatrix} -s\theta & -c\theta s\phi & c\theta c\phi & rc\theta c\phi \\ c\theta & -s\theta s\phi & s\theta c\phi & rs\theta c\phi \\ 0 & c\phi & s\phi & rs\phi \\ 0 & 0 & 0 & 1 \end{bmatrix} \quad (C.3)$$

$$\theta = \tan^{-1} \left( \frac{P_Y}{P_X} \right) \quad (C.4a)$$

$$\phi = \tan^{-1} \frac{P_Z c\theta}{P_X} \quad (C.4b)$$

$$r = \sqrt{P_X^2 + P_Y^2 + P_Z^2} \quad (C.4c)$$

There are two solutions,  $(\theta, \phi, r)$  and  $(\theta + \pi, \pi - \phi, r)$ .

### C.3 Articulated Manipulator

The articulated manipulator kinematics equations are derived with  $L_4 = 0$  in Table A.4.

$${}^B_F T = \begin{bmatrix} s_1 & c_1 s_{23} & c_1 c_{23} & L_1 c_1 + L_2 c_1 c_2 + L_3 c_1 c_{23} \\ -c_1 & s_1 s_{23} & s_1 c_{23} & L_1 s_1 + L_2 s_1 c_2 + L_3 s_1 c_{23} \\ 0 & -c_{23} & s_{23} & L_2 s_2 + L_3 s_{23} \\ 0 & 0 & 0 & 1 \end{bmatrix} \quad (C.5)$$

$$\theta_1 = \tan^{-1} \left( \frac{P_Y}{P_X} \right) \quad (C.6a)$$

$$(\theta_2 + \theta_3)_{1,2} = 2 \tan^{-1} \left[ \frac{-F \pm \sqrt{E^2 + F^2 - G^2}}{G - E} \right] \quad (C.6b)$$

$$\theta_2 = \tan^{-1} \left[ \frac{P_Z - L_3 s_{23}}{(P_X c_1 + P_Y s_1 - L_1) - L_3 c_{23}} \right] \quad (C.6c)$$

$$\theta_3 = (\theta_2 + \theta_3) - \theta_2 \quad (C.6d)$$

where:

$$E = 2L_3(P_X c_1 + P_Y s_1 - L_1)$$

$$F = 2L_3 P_Z$$

$$G = L_2^2 - L_3^2 - (P_X c_1 + P_Y s_1 - L_1)^2 - P_Z^2$$

Equation C.6a has two solutions,  $\theta_1$  and  $\theta_1 + \pi$ . Due to the length  $L_1$ , the quadrant-specific inverse tangent solution for  $\theta_1$  is valid (assuming the command is within the manipulator workspace) but the second solution exists only if the radicand in Eq. C.6b is non-negative. Each viable  $\theta_1$  has two associated  $\theta_2$  and  $\theta_3$  values. Thus, there are either two or four solutions.



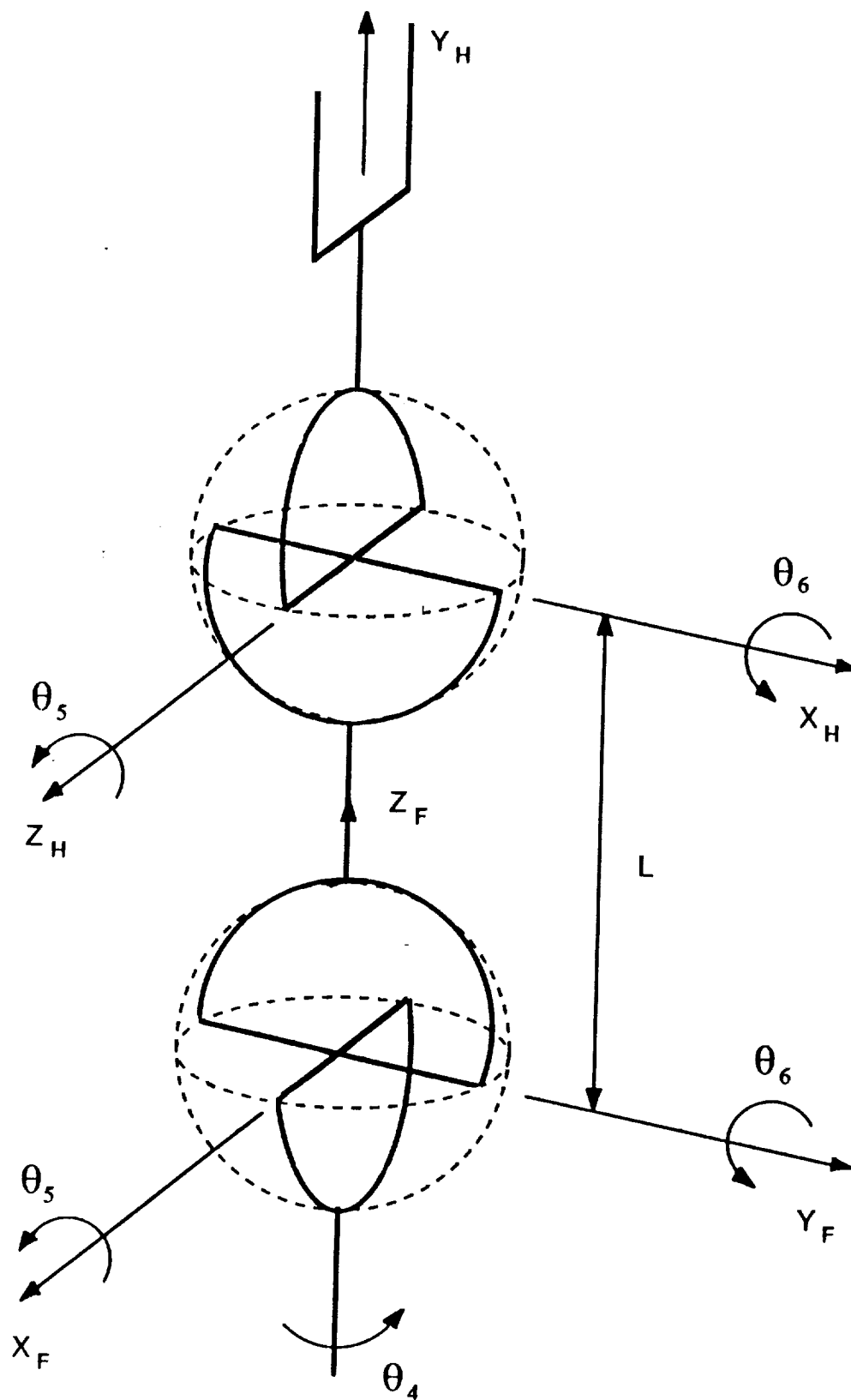


Figure 1  
Double Universal Joint Wrist  
Kinematic Diagram

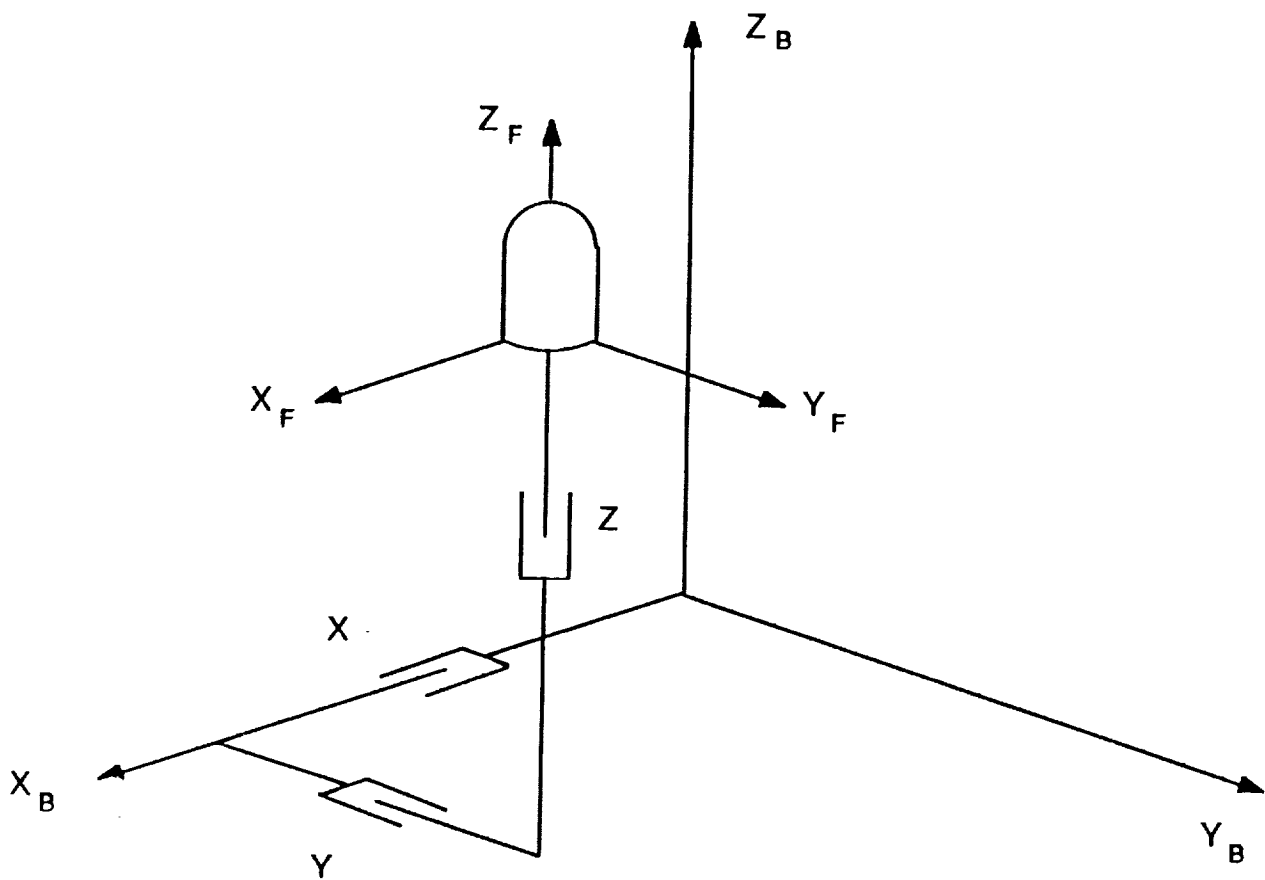


Figure 2a  
Cartesian Arm with  
Double Universal Joint Wrist

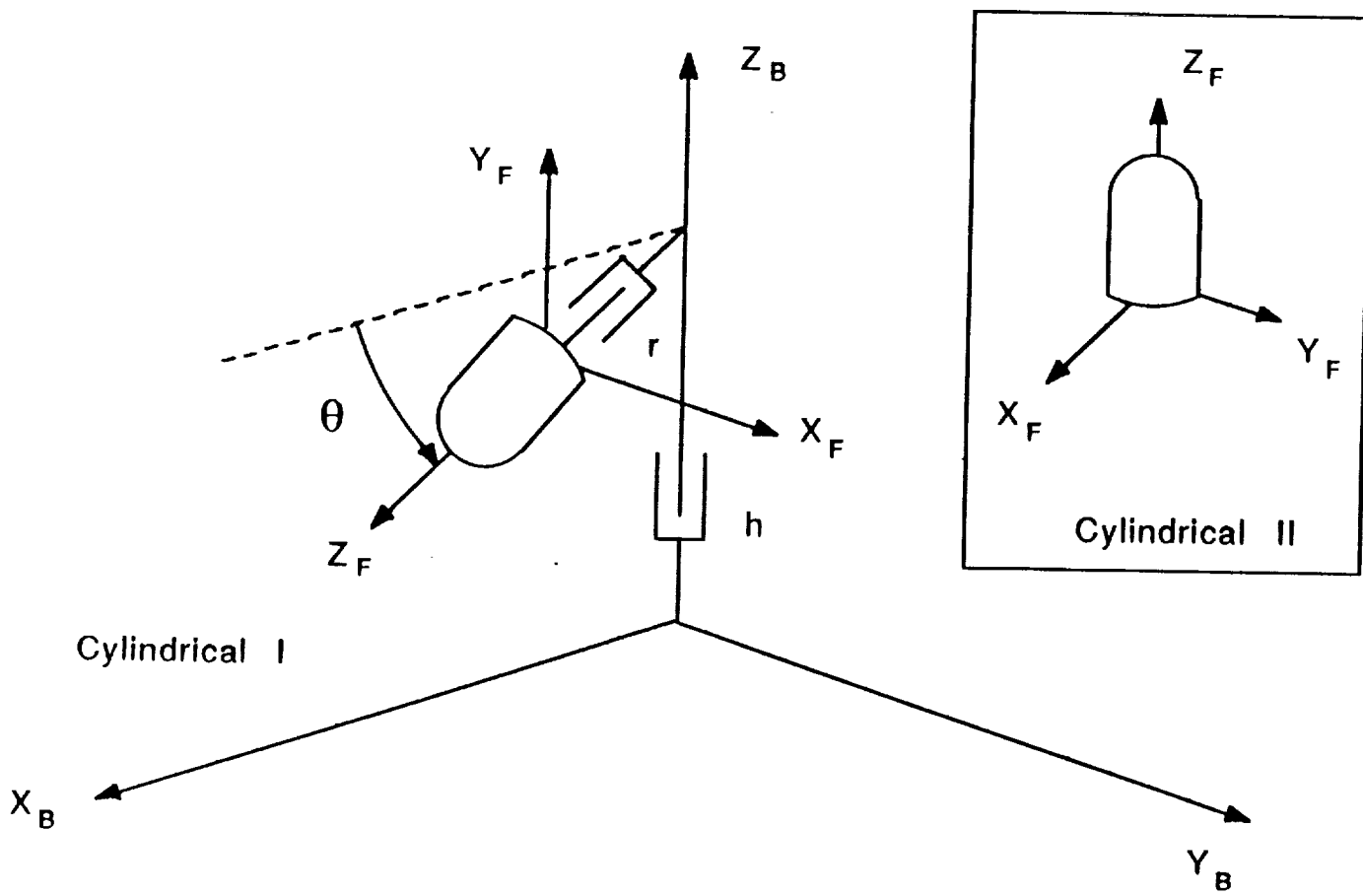


Figure 2b  
Cylindrical Arm with  
Double Universal Joint Wrist

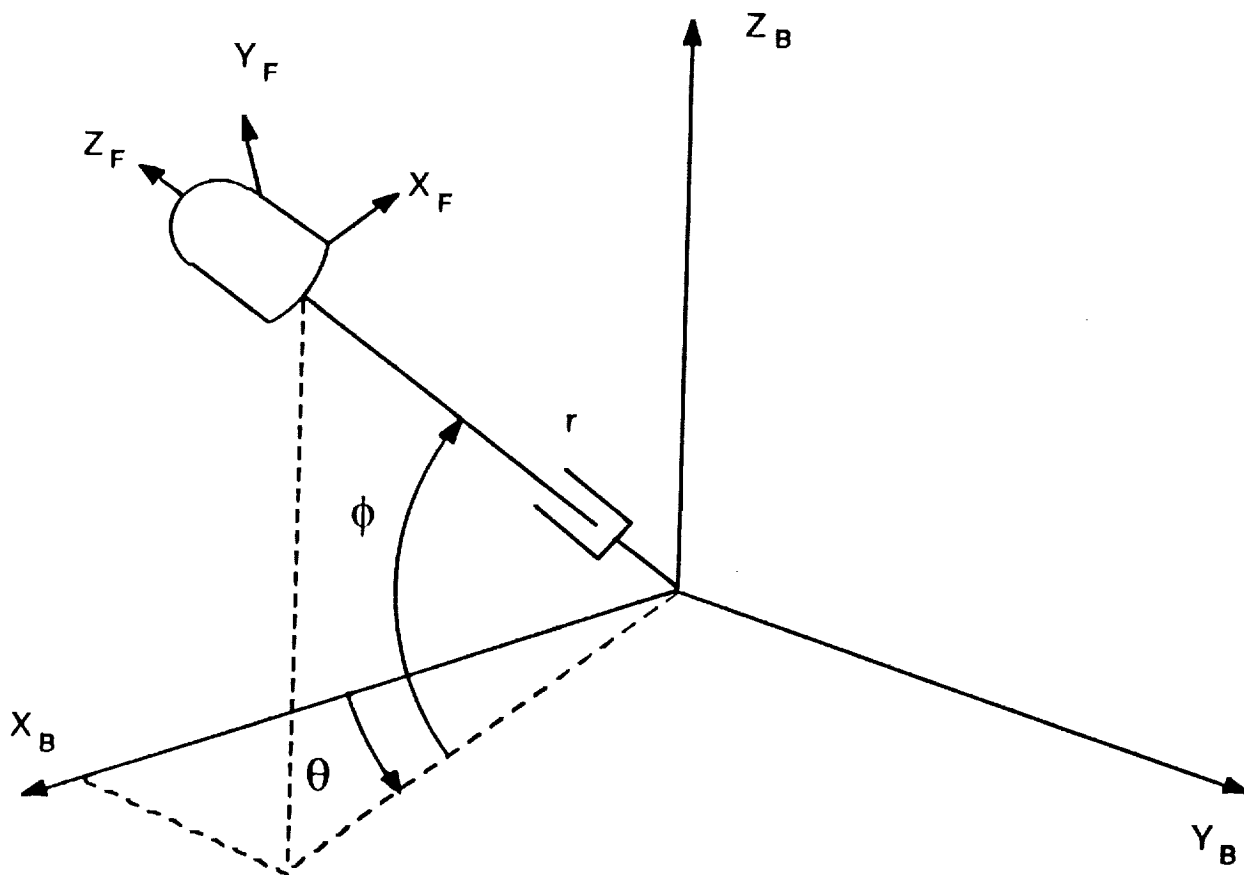


Figure 2c  
Spherical Arm with  
Double Universal Joint Wrist

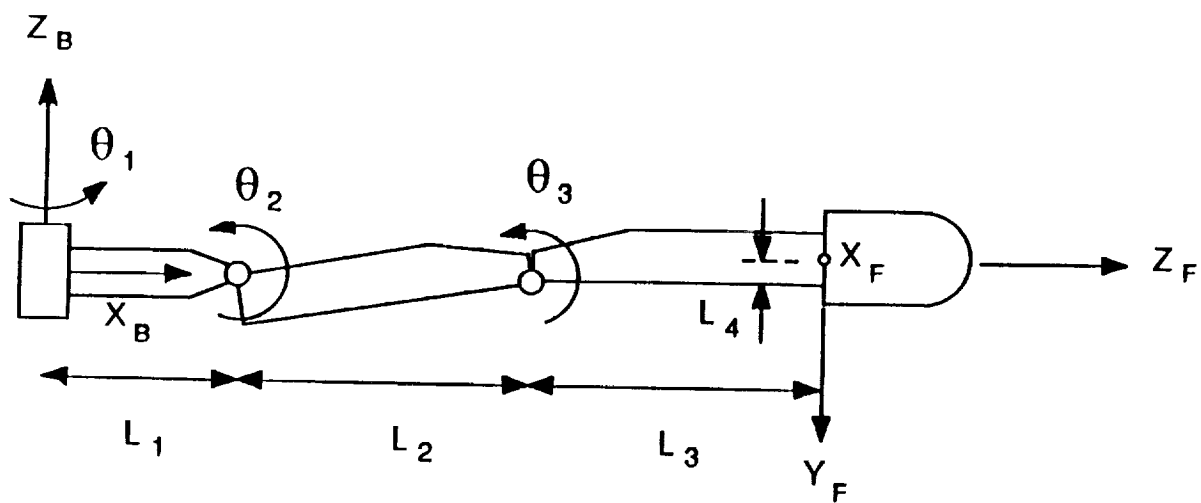


Figure 2d  
Articulated Arm with  
Double Universal Joint Wrist

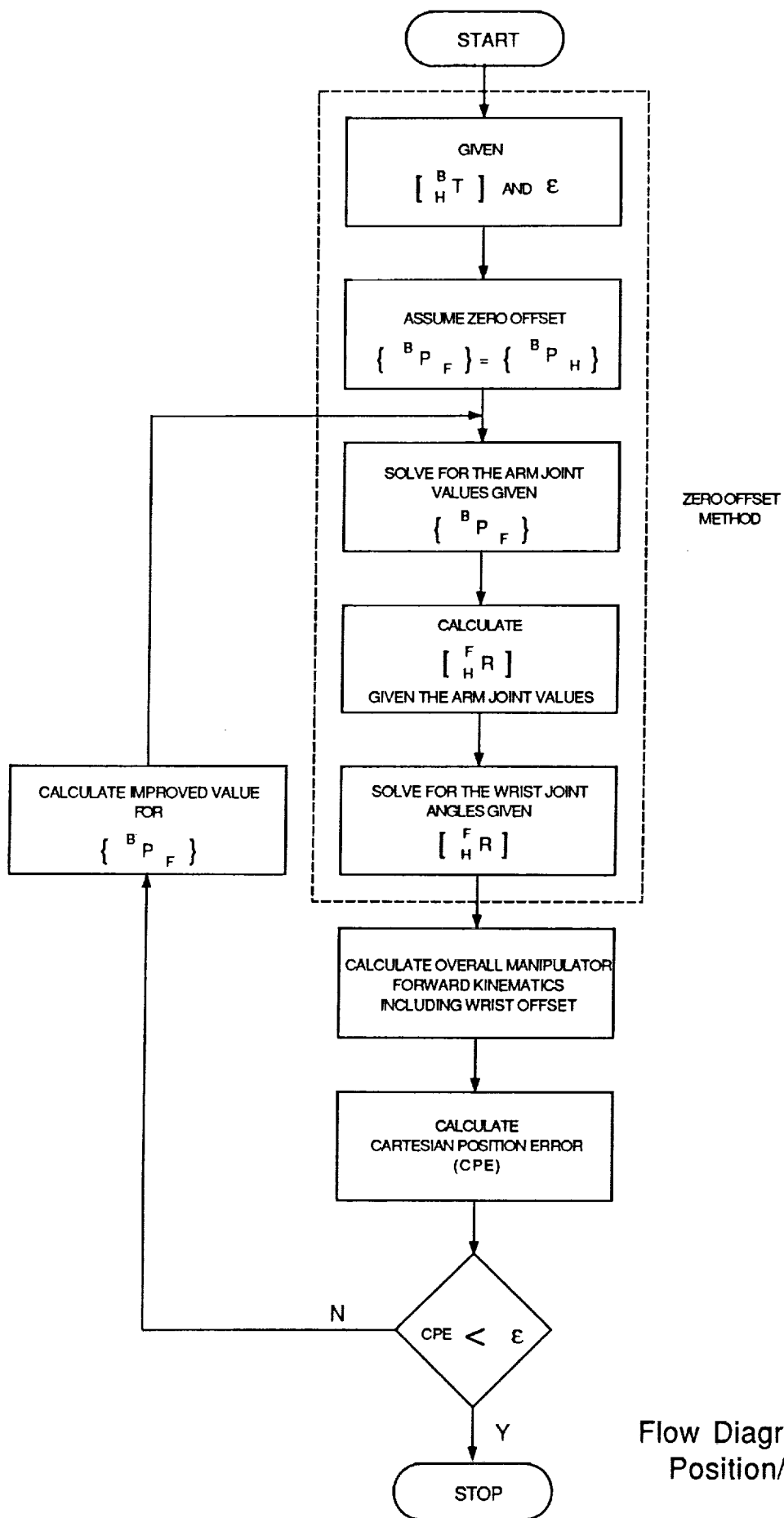


Figure 3  
Flow Diagram for Zero Offset and  
Position/Orientation Methods

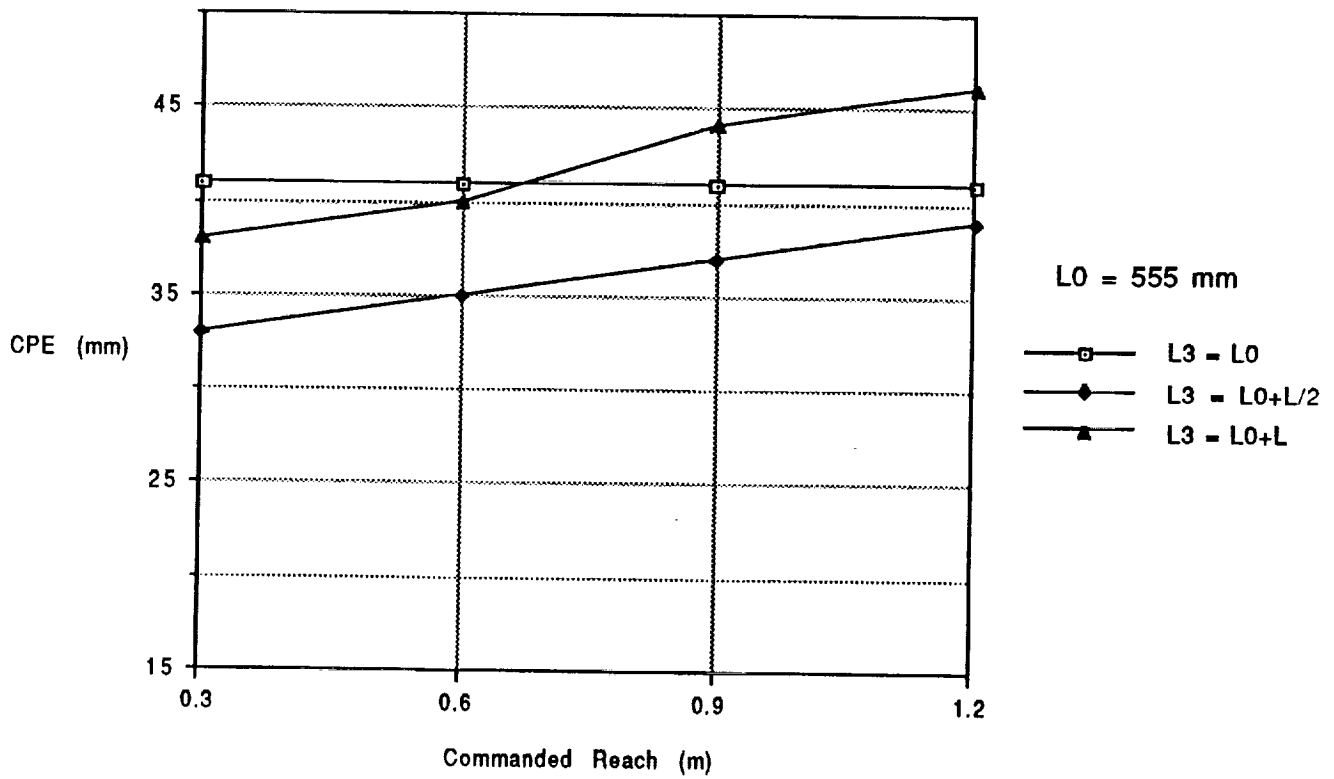


Figure 4  
Effect of Assumed Wrist Location ( $L3$ )  
on Cartesian Position Error (CPE) using  
Zero Offset Method for Articulated Arm

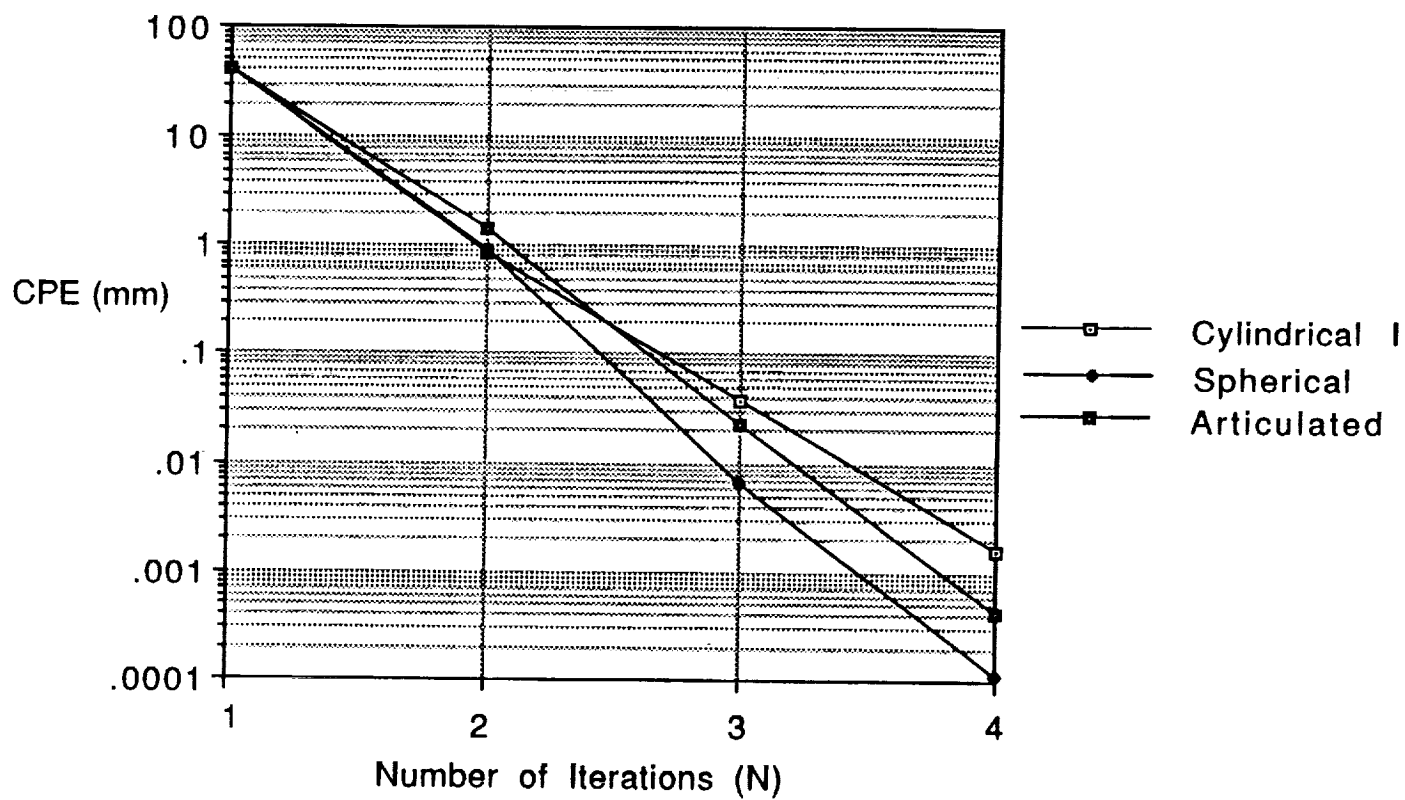


Figure 5  
Convergence of Cartesian Position Error (CPE)  
using the Position/Orientation Iteration Method



REPORT DOCUMENTATION PAGE			Form Approved OMB No. 0704-0188	
Public reporting burden for this collection of information is estimated to average 1 hour per response, including the time for reviewing instructions, searching existing data sources, gathering and maintaining the data needed, and completing and reviewing the collection of information. Send comments regarding this burden estimate or any other aspect of this collection of information, including suggestions for reducing this burden, to Washington Headquarters Services, Directorate for Information Operations and Reports, 1215 Jefferson Davis Highway, Suite 1204, Arlington, VA 22202-4302, and to the Office of Management and Budget, Paperwork Reduction Project (0704-0188), Washington, DC 20503.				
1. AGENCY USE ONLY (Leave blank)	2. REPORT DATE March 1992	3. REPORT TYPE AND DATES COVERED Technical Memorandum		
4. TITLE AND SUBTITLE The Double Universal Joint Wrist on a Manipulator: Solution of Inverse Position Kinematics and Singularity Analysis		5. FUNDING NUMBERS 595-11-22-01		
6. AUTHOR(S) Robert L. Williams II				
7. PERFORMING ORGANIZATION NAME(S) AND ADDRESS(ES) NASA Langley Research Center Hampton, VA 23665-5225		8. PERFORMING ORGANIZATION REPORT NUMBER		
9. SPONSORING / MONITORING AGENCY NAME(S) AND ADDRESS(ES) National Aeronautics and Space Administration Washington, DC 20546-0001		10. SPONSORING / MONITORING AGENCY REPORT NUMBER NASA TM-104212		
11. SUPPLEMENTARY NOTES				
12a. DISTRIBUTION / AVAILABILITY STATEMENT  Unclassified - Unlimited  Subject Category 63		12b. DISTRIBUTION CODE		
13. ABSTRACT (Maximum 200 words)  The double universal joint robot wrist can eliminate singularities which limit the performance of existing industrial robot wrists. Unfortunately, this singularity-free wrist has an offset which prevents decoupling of the position and orientation in the manipulator inverse kinematics problem. Closed form solutions are difficult, if not impossible, to find. This paper presents three methods to solve the inverse position kinematics position problem of the double universal joint wrist attached to a manipulator. Several manipulators are used to demonstrate the solution methods. A singularity analysis is present for the double universal joint wrist attached to these manipulator arms. While the double universal joint wrist standing alone is singularity-free in orientation, the singularity analysis indicates the presence of coupled position/orientation singularities of certain manipulators with this wrist. The methods of this paper can be implemented in a real-time controller for manipulators with the double universal joint wrist. Such mechanically dextrous systems could be used in tele robotic and industrial applications, but further work is required to avoid the singularities.				
14. SUBJECT TERMS Double Universal Joint Wrist, Robot Wrist, Manipulator, Singularity, Singularity-free, Kinematics.			15. NUMBER OF PAGES 39	
			16. PRICE CODE A03	
17. SECURITY CLASSIFICATION OF REPORT Unclassified	18. SECURITY CLASSIFICATION OF THIS PAGE Unclassified	19. SECURITY CLASSIFICATION OF ABSTRACT Unclassified	20. LIMITATION OF ABSTRACT	

